



www.sciencemag.org/cgi/content/full/1171085/DC1

Supporting Online Material for

Apicomplexan Parasites Co-Opt Host Calpains to Facilitate Their Escape from Infected Cells

Rajesh Chandramohanadas, Paul H. Davis, Daniel P. Beiting, Michael B. Harbut, Claire Darling, Geetha Velmourougane, Ming Yeh Lee, Peter A. Greer, David S. Roos, Doron C. Greenbaum*

*To whom correspondence should be addressed. E-mail: dorong@upenn.edu

Published 2 April 2009 on *Science Express*
DOI: 10.1126/science.1171085

This PDF file includes:

Materials and Methods
Figs. S1 to S6
Table S1
References

SUPPORTING ONLINE MATERIAL

Materials and Methods

Figs. S1 to S6

Table S1

References

Materials and Methods

Reagents and Antibodies

DCG04 was synthesized as reported previously (S1). Streptavidin-HRP was purchased from Vector Labs, and Fluo-4-AM and SYTOX-Green from Invitrogen. Purified human calpain-1 was purchased from Sigma, and calpastatin domain I from EMD Chemicals. Commercially available antibodies were obtained from the following sources: anti-GFP, anti-lamin A/C from Abcam; anti-band 4.9 from BD Biosciences; anti-ankyrin-1, anti-GAPDH, anti-flotillin, and anti-stomatin from Santa Cruz; and anti-band 3 and anti-calpain-1 from Sigma. Additional antibodies were kindly provided by: A. Holder (National Institute for Medical Research, UK), anti-*P. falciparum* merozoite surface protein-1 (MSP1); M. Klemba (Virginia Tech, USA), anti-*P. falciparum* plasmepsin II; and D. Speicher (Wistar Institute, USA), anti- α and β -spectrin. See below for other reagents.

Growth and maintenance of *P. falciparum* cultures

Strain 3D7 *Plasmodium* parasites were cultured in human red blood cells under standard conditions (S2), and replication was tightly synchronized by a serial treatments with D-sorbitol to lyse trophozoite- and schizont-infected RBCs. The remaining ring-stage parasites were cultivated to yield schizonts (~42 hr post-infection), which were selectively purified using a Miltenyi Biotec magnetic separator (S3). Cultures were staged by microscopy of Giemsa-stained blood smears.

Fractionation of *P. falciparum* infected erythrocytes

6×10^7 RBCs harboring schizont stage *P. falciparum* expressing cytosolic GFP were magnet-purified, incubated 10 min on ice with either 0.004% saponin, or 0.02% saponin, and centrifuged to isolate the soluble supernatant (S4). Pellets were further extracted in 0.5% Triton X-100/PBS. After gel electrophoresis and transfer to PVDF membranes, samples were probed with anti-GFP, anti-stomatin, anti-MSP1, or anti-plasmepsin II; see Fig. S1.

DCG04 profiling of extracellular protease activities during egress

Schizont stage parasites produced by serial sorbitol synchronization and magnet purification, were treated in culture with 3 μ M DCG04, synthesized as previously described (S1). The morphology of DCG04-treated parasites was compared with DMSO-treated controls at 48 and 60 hr by examining Giemsa stained blood smears on an Olympus compound microscope. Images were captured and processed using a Spot RT Color digital camera and Spot Advanced Image analysis software (Diagnostic Instruments); Fig. 1A.

To profile active targets of DCG04 during parasite egress, synchronized cultures (10 ml per sample) were treated with DCG04 for 2 hr at 24, 32, 40 or 48 hr post-infection, corresponding to early trophozoites, late trophozoites, early schizonts, and late schizonts. Infected RBCs were collected by centrifugation, and extraparasitic material (including both membranous and soluble contents of the host RBC/PV), separated from parasite cells by treatment with 0.02% saponin. This material was further fractionated into membrane and soluble components by ultracentrifuga-

tion for 2 hr at 200,000 x g at 4°C. Equivalent amounts of the membrane and soluble material were analyzed by immunoblotting using streptavidin-HRP. As controls for protein loading and effective separation of RBC membranes and cytoplasm, the PVDF membrane was stripped and re-probed using an anti-band 4.9 and anti-calpain-1 (Fig. 1B).

Identification of extraparasitic cysteine proteases involved in parasite egress

DCG04-labeled proteins were obtained from 1.5 liters of synchronized, purified schizonts (5% parasitemia) harvested over two weeks in batches of 300 ml. Infected RBCs were treated for 2 hr with 3 μ M DCG04 (*SI*) at ~46 hr post-infection, and extraparasitic material fractionated using saponin as described above. The extraparasitic membrane pellet was solubilized in extraction buffer (0.5% Triton X-100 + 0.2% SDS in PBS), and biotinylated proteins purified on streptavidin-agarose beads (Pierce). Affinity purified proteins were solubilized in Laemmli buffer, and ~95% of this material was separated on a 4-12% SDS-PAGE gel and stained with colloidal Coomassie; the remaining 5% was resolved on a second gel and analyzed by western blotting for biotinylated proteins using streptavidin-HRP. Stained bands corresponding the DCG04-labeled proteins on the western blot were excised, digested with trypsin (Promega) and peptides were extracted for analysis by mass spectrometry. Mass spectrometry was performed on a LTQ mass spectrometer (Thermo Electron), using a 5-90% gradient (flow rate 200 nl/min). MS/MS data was analyzed using SEQUEST and PeptideProphet as an automated method to assign peptides to MS/MS spectra. Proteins with at least two matching peptides were identified as positive 'hits' (Table S1).

Calpain-1 immunodepletion, reconstitution and calpastatin loading of RBCs

Erythrocyte ghosts were prepared by hypotonic lysis as previously described (*S5*), with minor modifications. RBCs were washed twice with PBS and allowed to lyse in 5 mM K_2HPO_4 containing 1 mM ATP (pH 7.4). To immunodeplete cytosolic (inactive) calpain as it is released from lysed RBCs, anti-calpain-1 was pre-conjugated to Protein G-Sepharose (Upstate/Millipore), and incubated with ghosts for 1 hr on ice with gentle mixing. This slurry was separated by centrifugation, and ghosts were resealed by gradual addition of 5X resealing buffer (475 mM KOAc, 25 mM Na_2HPO_4 , 25 mM $MgCl_2$, 237.5 mM KCl, pH 7.5) over 1 hr at 37°C. Parallel studies were carried out using anti-flotillin, and mock treated RBCs were incubated with Sepharose G beads without antibodies. Titration of anti-calpain-1 coupled to protein G-Sepharose indicated that complete immunodepletion was obtained using 1 μ g antibody per 10^6 erythrocytes. For reconstitution studies, 30 ng/ μ l purified human calpain-1 was added to hypotonically lysed, calpain-1 immunodepleted RBCs prior to resealing. Mock-treated RBC ghosts were also resealed in the presence of 1 μ M calpastatin domain I. Western blotting with anti-calpain-1 confirmed immunodepletion and reconstitution; anti-band 4.9 and anti-stomatatin were used as loading controls (Fig. 2A).

Monitoring calpain activation and membrane binding

Five equal aliquots of freshly washed RBCs were hypotonically lysed in 5 mM phosphate buffer and resealed to yield the following samples: mock-treated, flotillin-depleted, calpain-depleted, calpastatin-loaded or calpain-complemented, as described above. After 30 min incubation at RT with DCG04 (5 μ M) in presence of 2 mM $CaCl_2$ and 5 mM DTT, membrane fractions were prepared from each sample by ultracentrifugation (2 hr at 200,000 x g). Equal amounts of solubilized protein from each sample was separated by SDS-PAGE, transferred to PVDF membrane, and probed for biotin using streptavidin-HRP, revealing DCG04 labeling of active calpain. As a loading control, the same immunoblots were probed with anti-stomatatin (Fig 1B).

Analysis of calpain-mediated egress from resealed RBCs

To assay for calpain function during egress, resealed RBCs were prepared as described above. Schizont stages were isolated from 10 ml parasite culture by magnet purification ~40 hr after sorbitol synchronization, and added to either mock-treated, flotillin-depleted, calpain-depleted, calpastatin-loaded or calpain-reconstituted resealed RBCs to a final hematocrit of 4%. Parasites invaded resealed erythrocytes normally (Fig. S2A), and progress through the intraerythrocytic cycle was monitored by smears (Fig. 2B). Schizont-stage parasites were followed to assess egress and the establishment of rings in newly-infected RBCs from ~46-60 hr post-infection.

Flow cytometry was exploited for quantitative evaluation of *P. falciparum* development in resealed RBCs, as previously described (S6). Beginning at 47.5 hr post-infection, culture aliquots were harvested at 90 min intervals, fixed in 4% formaldehyde/0.0075% glutaraldehyde in PBS, permeabilized 10 min in 0.25% Triton X-100, and stained 5 min with 5 μ M SYTOX-Green at RT. 10^6 events were collected per sample using a LSRII flow cytometer (Becton Dickinson), and analyzed using FlowJo 8.7 software (TreeStar), gating to exclude debris defined by scatter characteristics, and uninfected RBCs based on low fluorescence; rings and trophozoites were distinguished from schizonts based on DNA content (Fig 2C).

Calcium studies

Late schizont stage infected RBCs (~ 46 hr post-infection) were magnet-purified and loaded with 5 μ M Fluo-4 AM for 30 min at 37°C, washed with incomplete media, and stained 5 min in DAPI. Parasitized erythrocytes were visualized by UV fluorescent microscopy on a Zeiss Axioskop, and composite images prepared using Photoshop 6.0.1 (Adobe); Fig. S5A.

Schizont stage infected RBCs (~40 hr post-infection) were also treated with increasing concentrations of the cell-permeable Ca^{2+} chelator EGTA-AM, in parallel with DMSO-treated controls. Smears were taken ~7 hr and 20 hr later, fixed in methanol and stained with Giemsa. Images were captured on an Olympus BX60 compound microscope, and processed using a Spot RT Color digital camera and Spot Advanced Image analysis software (Diagnostic Instruments). Parallel aliquots were collected at 60 hr post-infection, fixed with paraformaldehyde and stained with 5 μ M SYTOX green for flow cytometry to establish a dose-response curve (Fig. S5B).

Evaluation of potential calpain-1 targets in vitro and in intact RBCs during parasite development and egress

Spectrin/actin was purified from hypotonically lysed RBCs as previously reported (S7), and treated with 200 ng purified calpain-1 in presence of CaCl_2 for 30 min at 37°C. Negative controls were conducted without calcium, or in the presence of DCG04, calpastatin or EGTA. Each sample was then separated by SDS-PAGE and stained with colloidal Coomassie (Fig. S4A).

Magnet-purified schizont stage parasites were allowed to infect mock-treated, calpain-depleted, calpastatin-loaded and calpain-complemented RBCs, and Giemsa smears were used to monitor parasite growth in the following cycle. Once mock-treated parasites began to rupture the host RBCs, each sample was incubated in 5% sorbitol for 10 min at 37°C, in order to selectively lyse and release infected RBC membrane material. After parasites were removed by a low speed spin, supernatants were ultracentrifuged to pellet the parasitophorous vacuole and RBC membranes. Equal amounts of total protein from each sample were separated by SDS-PAGE and probed for cytoskeletal proteins using antibodies to ankyrin-1, band 3, stomatin, and anti- α and β -spectrin (Fig. S4B).

Growth and maintenance of *T. gondii* cultures

Wild type RH strain *Toxoplasma gondii* tachyzoites, and parasites constitutively expressing cytoplasmic luciferase (*S11*) or YFP (*S13*) were cultivated in confluent monolayers of human foreskin fibroblasts (HFF), human U-2 OS cells, or mouse embryonic fibroblasts (MEF; kindly provided by P. Greer (*S8*)). Cells were grown to confluence in Dulbecco's modified Eagle's medium containing 10% newborn bovine serum (D10), replaced upon infection with minimal essential medium containing 1% dialyzed fetal bovine serum (ED1), as previously described (*S9*).

Calpain siRNA knock-downs

Expression of calpain-1 (CAPN1; CAPN1_10; Qiagen), calpain-2 (CAPN2; CAPN2_4; Qiagen), the common small regulatory subunit for both of these proteins (CAPNS1; 'Oligo#1' CAPNS_1_1; 'Oligo#2', CAPNS_1_3; Qiagen), or lamin A/C (positive control for siRNA activity; Dharmacon) was knocked-down using siRNAs. siRNAs were added at a final concentration of 20 nM in 35 mm dishes, along with 10^6 U-2 OS cells in culture medium lacking phenol red but containing 25 mM HEPES (HT-D10), and reverse-transfection was carried out using HiPerfect reagent according to the manufacturer's instructions. Transcript levels of targeted genes were determined in uninfected cultures at 48 hr post-transfection, by quantitative real-time PCR using the ABI Power SYBR master mix (Applied Biosystems 7000), according to the manufacturer's instructions. The following qPCR primers were used for amplification: CAPNS1 Forward: ACC TGG ATT TGT CCA GTG CCA TCT, Reverse: GCC ATG TTC CGT GCC TTC AAA TCT; Human GAPDH Forward: TGC ACC ACC AAC TGC TTA GC, Reverse: GGC ATG GAC TGT GGT CAT GAG; CAPN1 Forward: AGGAAGGCAGCTTTCGCTTGTT, CAPN1 Reverse: GTTTATAGTCTGCAGGCAAGGCCA; CAPN2 Forward: ATCCTGCGC-TTGATCAACTGAACC, CAPN2 Reverse: ATGGACAGACACTAGTGGTGGTGA. Transfected host cells were inoculated with 10^5 YFP-expressing *T. gondii* tachyzoites (*S13*) 24 hr post-transfection, and imaged at 56 hr post-infection.

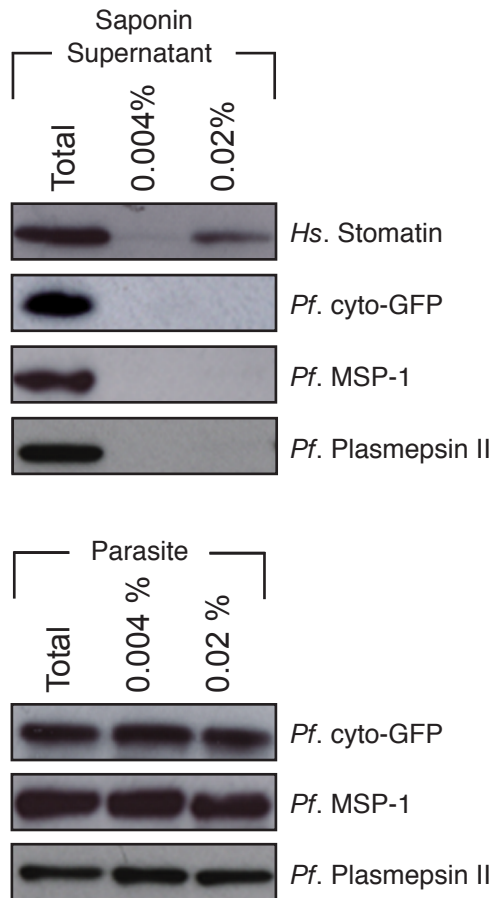
***T. gondii* invasion, replication, and egress in CAPNS1 knockout and knockdown cultures**

Invasion of wild-type, CAPNS1 knockout, and CAPNS1-complemented MEF host cells by *T. gondii* was measured by plating 4×10^4 cells/well in 96-well flat-bottom opaque plates in HT-D10 media. 24 hr after plating, 4×10^4 *T. gondii* parasites expressing a transgenic luciferase reporter (*S11*) were added to each well, incubated for 4 hr at 37°C, and washed twice with PBS to remove extracellular parasites. 50 μ l Britelite buffer (Perkin-Elmer) was added to 50 μ l PBS, and luminescence values were measured on an Analyst HT plate reader (Molecular Devices). See Fig. 3D.

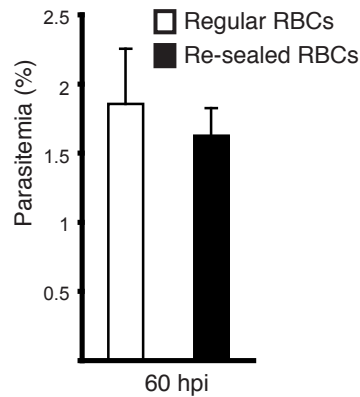
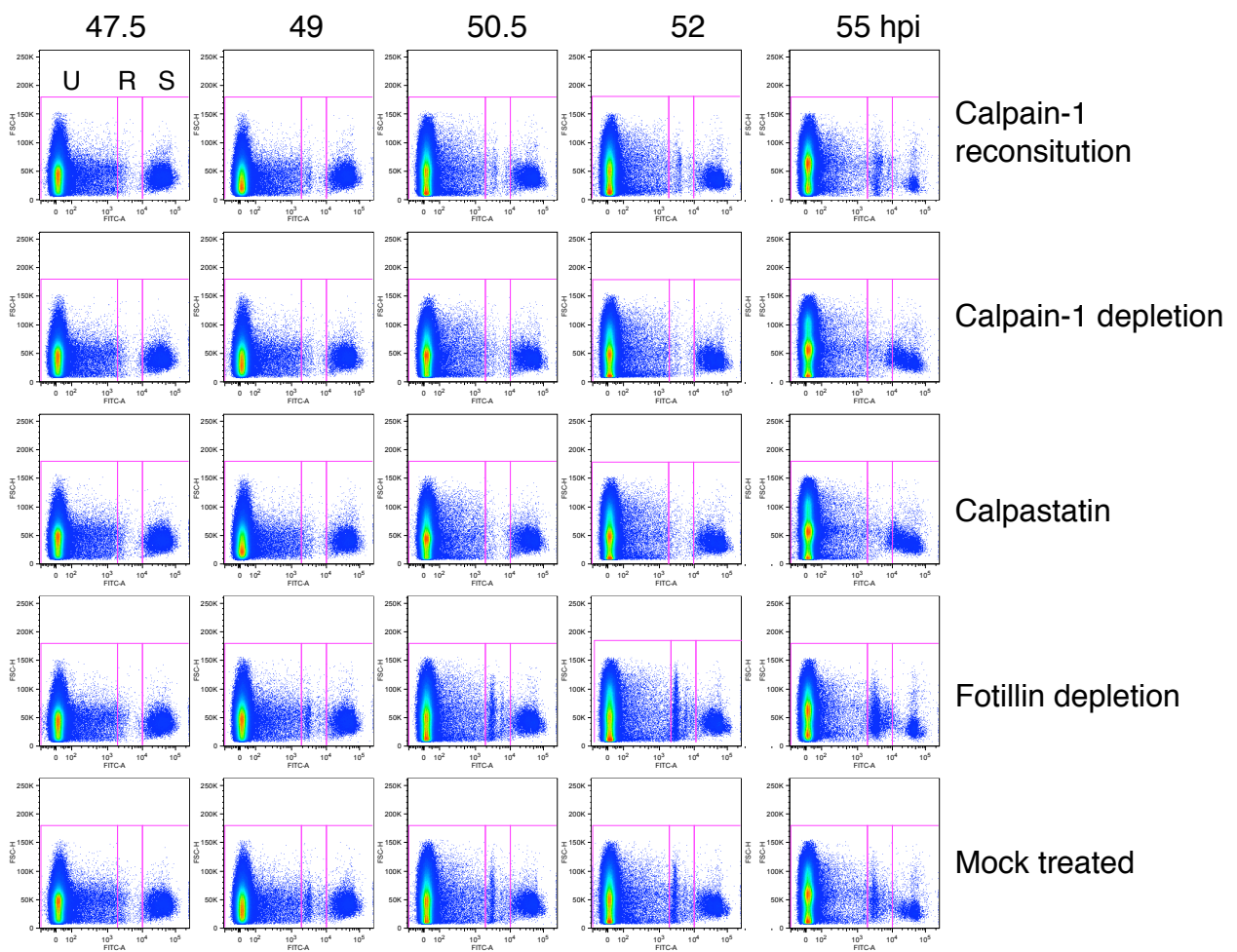
Intracellular parasite growth was measured as previously described (*S12*), by counting the number of parasites per parasitophorous vacuole at 24, 36 and 48 hr post-infection (prior to egress from the initial host cell). Confluent monolayers of $\sim 5 \times 10^5$ wild-type, CAPNS1 knockout, and CAPNS1-complemented MEF host cells in 60 mm dishes were infected with 10^6 *T. gondii* parasites. At least 100 vacuoles were counted per time point, and doubling rates were determined as the average \log_2 number of parasites per vacuole (Fig. 3E).

T. gondii growth and replication was also assessed over the longer term by plaque assays (*S9*), inoculating confluent monolayers of wild-type, CAPNS1 knockout, and CAPNS1-complemented MEF cells in T25 flasks with 10^5 *T. gondii* parasites in 60 ml ED1 media containing 40 mM HEPES buffer. Flasks were incubated undisturbed for 7d at 37°C, followed by methanol fixation and staining with crystal violet. Images were captured using a desktop scanner (Epson) and plaque sizes calculated using ImageJ software (Fig. 3F, 3G).

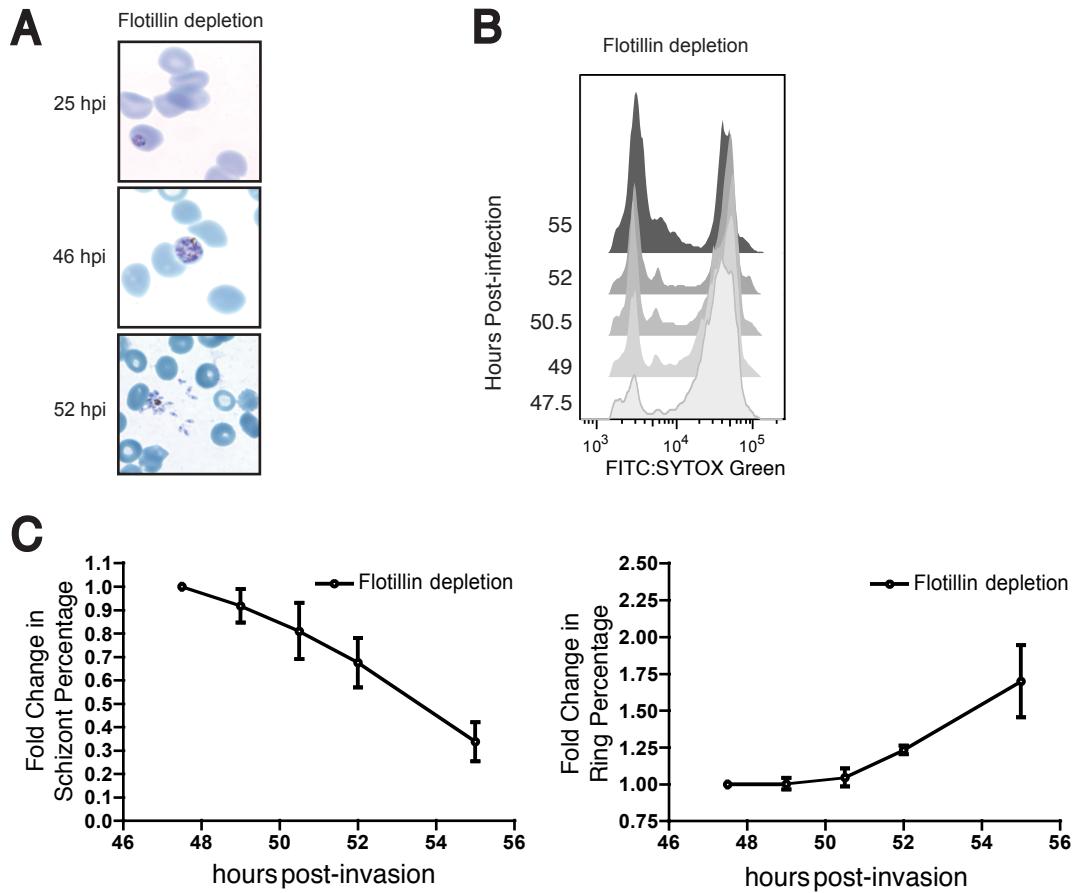
Active egress by living *T. gondii* parasites was imaged in real time using YFP transgenic parasites (*S13*) inoculated into 35 mm glass bottom culture dishes containing confluent monolayers of wild-type, CAPNS1 knockout, or CAPNS1-complemented MEF host cells (Fig. 3C), or U2OS cells following siRNA-mediated knockdowns as described above (Fig. 3A). Infection was carried out at a multiplicity of infection (MOI) of 1:1, and parasite egress was imaged ~56 hours post invasion using a Leica DMI6000B microscope equipped with a 40X DIC objective.



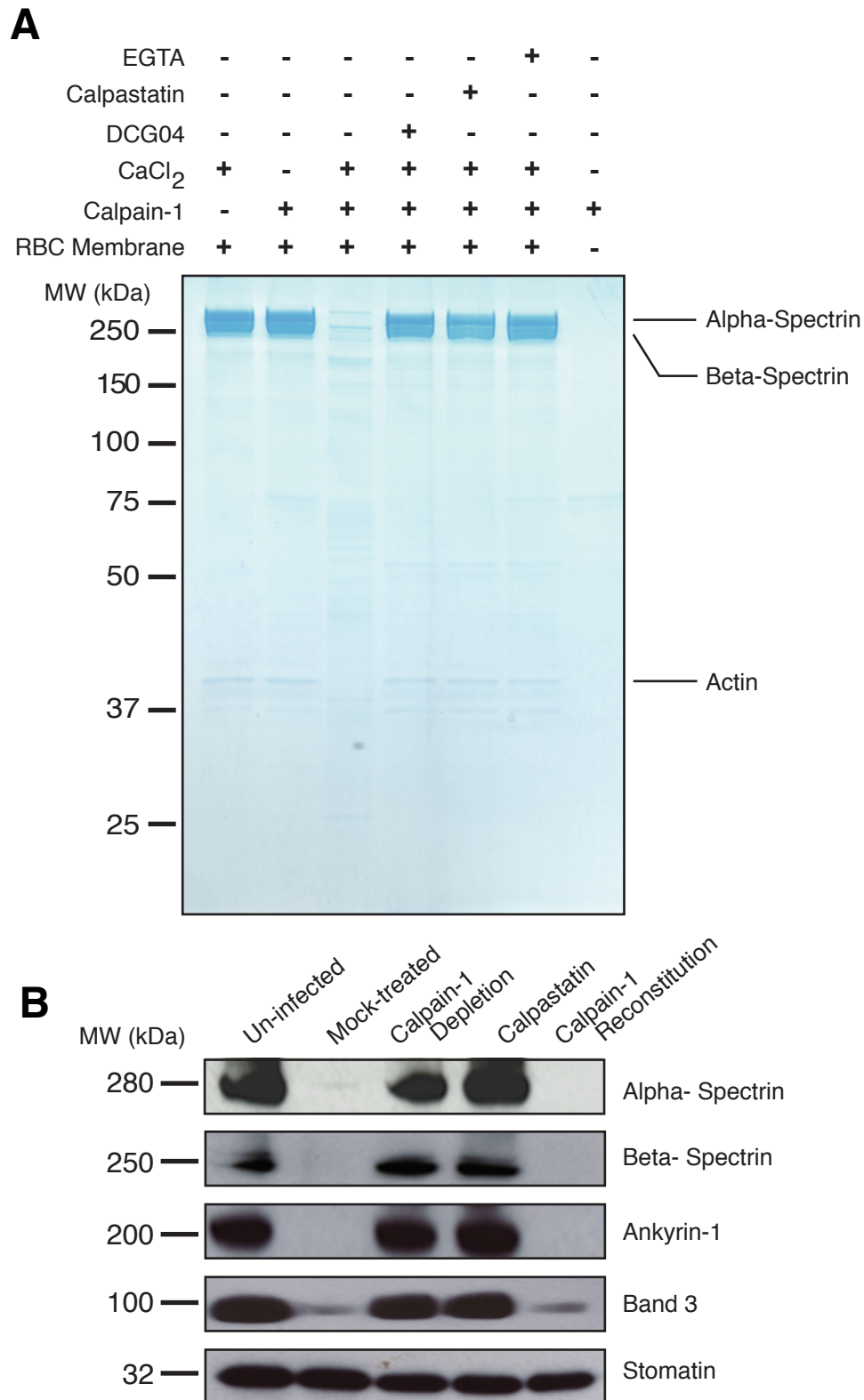
Supplementary Fig. 1. Fractionation of parasites from the infected erythrocytes using saponin. Schizont stage parasites expressing cytosolic GFP were enriched on a magnetic column and treated with either 0.004 or 0.02% saponin in PBS for 5 min on ice, followed by centrifugation. Equivalent amounts of the supernatant and Triton X-100 extracted pellets were resolved by SDS-PAGE, transferred to PVDF membranes, and immunoblots probed with antibodies against GFP, the digestive vacuole marker plasmepsin-II, the parasite membrane marker MSP-1, and the RBC membrane marker stomatin. No detectable parasite contamination was observed in the supernatant after permeabilization with 0.02% saponin, but the majority of erythrocyte stomatin was recovered in this fraction.

A**B**

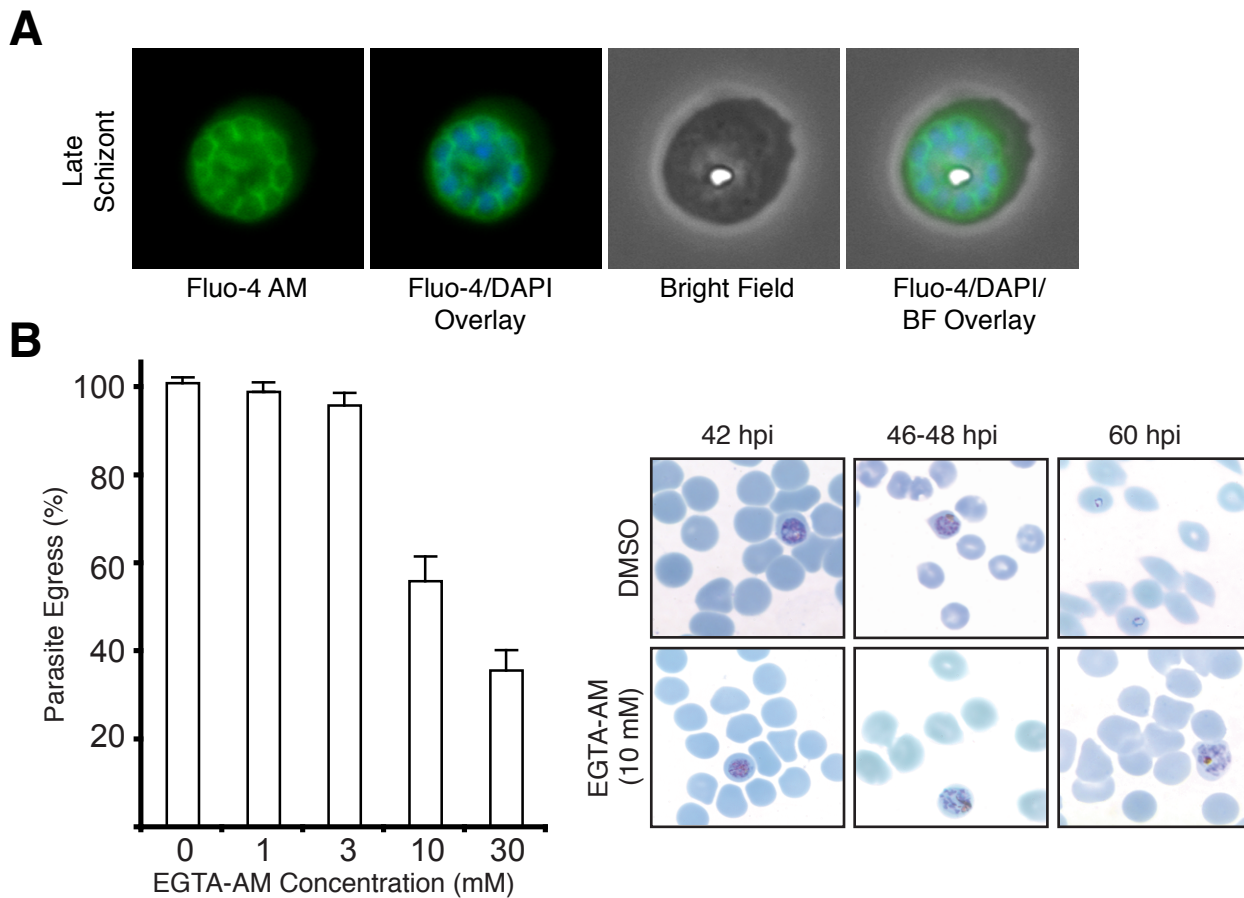
Supplementary Fig. 2. Infection and egress in resealed erythrocytes. (A) Magnet purified schizonts (42 hr post-infection) were added to either untreated RBC controls or mock-treated resealed RBCs, to at an initial parasitemia of 0.5%. After incubation for 18 hr, cultures were fixed in 4% paraformaldehyde and stained with SYTOX-Green to detect parasite DNA. Flow cytometry showed comparable levels of infection in control RBCs and resealed ghosts. (B) Flow cytometry data for parasite progression from the schizont stage infection onwards, in mock-treated, flotillin-depleted, calpastatin-loaded, calpain-depleted, or calpain-reconstituted RBCs. Boxes indicate gates used to define uninfected cells (U), ring-stages + trophozoites (R) or schizonts stages (S).



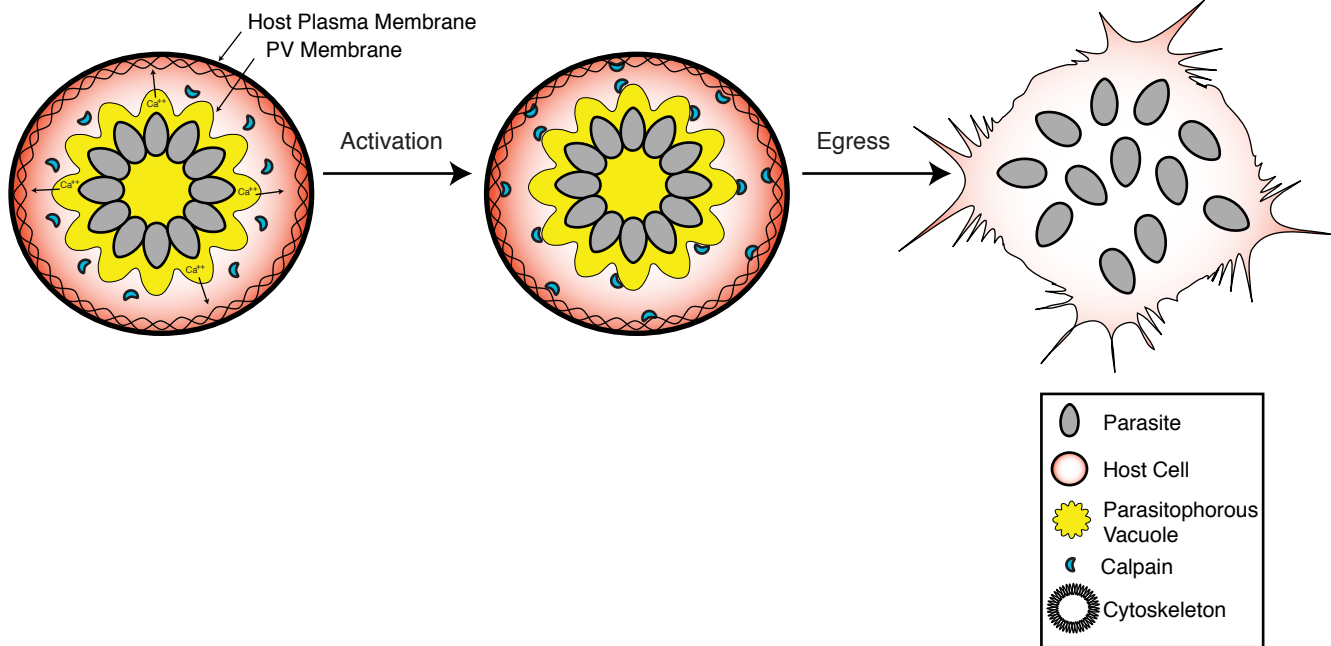
Supplementary Fig. 3. Parasite egress from anti-flotillin immunodepleted RBCs. RBCs resealed after flotillin immunodepletion were infected with magnet-purified schizonts. Normal egress was observed by both Giemsa-staining (A) and flow cytometry (B, C). Bars indicate standard error from 4 independent experiments.



Supplementary Fig. 4. Proteolysis of RBC cytoskeletal proteins by calpain-1. (A) Erythrocyte actin and α and β -spectrins were purified from RBCs, and 4 μ g aliquots incubated with purified human calpain-1 in the presence or absence of calpain inhibitors or CaCl₂, as indicated. All three proteins exhibited calcium-dependent proteolysis by calpain-1; proteolytic activity was blocked by DCG04, EGTA or calpastatin. (B) Proteolysis of the RBC cytoskeleton during parasite egress. Magnet-purified parasites were allowed to invade mock-treated, calpain-depleted, calpastatin-loaded or calpain reconstituted RBCs. Material released by 5% sorbitol treatment of schizont stage parasites was probed for the RBC membrane/cytoskeletal proteins α and β -spectrin, ankyrin-1, band 3 and stomatin. Extensive proteolysis was evident in mock-treated and calpain-1 reconstituted samples, but not calpain-immunodepleted or calpastatin treated parasites.



Supplementary Fig. 5. Calcium imaging and depletion during *P. falciparum* infection. (A) Late-stage schizonts loaded with 5 μ M Fluo-4-AM for 30 min at 37°C show a calcium signal in the parasitophorous vacuole during late schizogony, 48 hr post-infection (green). Parasite nuclei were counterstained with DAPI (blue) (B) Schizont stage infected erythrocytes were magnet-purified 42 hr post-infection and resuspended in cultures containing the cell-permeable calcium chelator EGTA-AM. Flow cytometry of formaldehyde-fixed SYTOX green-stained samples showed a dose-dependent effect of calcium depletion on parasite egress. Giemsa stained smears of infected RBCs treated with EGTA-AM were blocked in egress, while DMSO-treated controls ruptured the host cells and established new ring stage infection.



Supplementary Fig. 6. Model of calpain-dependent parasite egress. Late schizont stage *P. falciparum* schizonts (shown just prior to egress from the infected red blood cell) are suspected to mobilize calcium from the parasitophorous vacuole membrane, activating host cell calpain-1, which binds to RBC and parasitophorous vacuole membranes, proteolyzing cytoskeletal proteins such as spectrin and ankyrin, thereby weakening the membrane and facilitating parasite release.

	ID	Protein	MW (kDa)	Sequence Coverage	Peptides	Score	Peptides Identified
Calpain peptides							
Band A	CAN1_HUMAN	Calpain-1 catalytic subunit	81	42%	27	7009	R.ARELGLGR.HENAIK.Y R.HENAIKYLGDYEQLR.V K.YLGDYEQLRV.R.C K.TYGIKWK.R K.WKRPTLLSNPQFIVDGATR.T R.KAPSDLYQILK.A K.LVKGHAYSVTGAK.Q K.GHAYSVTGAK.Q R.GQVSLIR.M K.MEDGGEFWMFRDFMR.E R.GSTAGGCRNYPATFWVNPQFK.I R.NYPATFWVNPQFK.I K.RDFFLANASR.A R.DFFLANASR.A R.ARSEQFINLREVSTR.F R.SEQFINLREVSTR.F R.FRLPPGEYVVVPSTFEPNK.E K.EGDFVLR.F R.QLAGEDMEISVKELR.T R.SMVNLMDRDGNGK.L R.RNYSIFR.K R.NYSIFR.K R.KFDLDSGMSAYEMR.M K.SGMSAYEMR.M R.MAIESAGFKLNKK.L K.LNKKLYELIIR.Y R.LETMFR.F
Band B	CAN1_HUMAN	Calpain-1 catalytic subunit	81	21%	14	1496	R.ARELGLGR.H K.YLGDYEQLR.V K.WKRPTLLSNPQFIVDGATR.T R.KAPSDLYQILK.A K.QVNYRGQVSLIR.M R.GQVSLIR.M K.WNTLYEGTWR.R R.NYPATFWVNPQFK.I R.DFFLANASR.A R.ARSEQFINL.R.E R.ARSEQFINLREVSTR.F R.SEQFINL.R.E R.SEQFINLREVSTR.F R.FRLPPGEYVVVPSTFEPNK.E
Band C	CAN1_HUMAN	Calpain-1 catalytic subunit	81	18%	12	1216	R.ARELGLGR.H K.YLGDYEQLR.V K.RPTELLSNPQFIVDGATR.T R.KAPSDLYQILK.A K.APSDLYQILK.A K.GHAYSVTGAK.Q K.QVNYRGQVSLIR.M R.GQVSLIR.M R.NYPATFWVNPQFK.I R.DFFLANASR.A R.SEQFINLREVSTR.F R.FRLPPGEYVVVPSTFEPNK.E

Other Proteins Identified							
	ID	Protein	MW (kDa)	Sequence Coverage	Peptides	Score	
Band A	NSF_HUMAN	Vesicle-fusing ATPase	82	24%	8	898	
	SBP1_HUMAN	Selenium-binding protein 1	52	21%	5	893	
	TGM2_HUMAN	Protein-glutamine gamma-glutamyltransferase 2	77	16%	5	877	
	K6PL_HUMAN	6-phosphofructokinase, liver type	85	19%	5	804	
	TCPA_HUMAN	T-complex protein 1 subunit alpha	60	25%	10	860	
Band B	SBP1_HUMAN	Selenium-binding protein 1	52	22%	6	910	
	TCPA_HUMAN	T-complex protein 1 subunit alpha	60	25%	10	860	
	TCPG_HUMAN	T-complex protein 1 subunit gamma	60	19%	7	807	
	TCPZ_HUMAN	T-complex protein 1 subunit zeta	58	22%	7	634	
	TCPH_HUMAN	T-complex protein 1 subunit eta	59	27%	11	597	
Band C	SBP1_HUMAN	Selenium-binding protein 1	52	36%	12	1989	
	PRS6A_HUMAN	26S protease regulatory subunit 6A	49	21%	6	793	
	EM55_HUMAN	55 kDa erythrocyte membrane protein	52	19%	6	512	

Supplementary Table 1. MS identification of calpain-1. Mass spectrometry data for protein(s) affinity purified from DCG04-labeled infected erythrocyte membranes (Fig. 1). SEQUEST scores and tryptic peptides are shown for all protein ‘hits’ identified. Bands A-C represent three protein species separated on a SDS-PAGE gel. The DCG04-labeled peptide was not detected, presumably because the expected 3 kDa tryptic peptide is larger than the mass window employed for this experiment.

References

- S1. D. Greenbaum, K. F. Medzihradzky, A. Burlingame, M. Bogyo, *Chem Biol* **7**, 569 (2000).
- S2. W. Trager, J. B. Jensen, *Science* **193**, 673 (1976).
- S3. T. Staalsoe, H. A. Giha, D. Dodoo, T. G. Theander, L. Hviid, *Cytometry* **35**, 329 (1999).
- S4. P. Delplace, B. Fortier, G. Tronchin, J. F. Dubremetz, A. Vernes, *Mol Biochem Parasitol* **23**, 193 (1987).
- S5. S. C. Murphy *et al.*, *PLoS Med* **3**, e528 (2006).
- S6. A. E. Bianco, F. L. Battye, G. V. Brown, *Exp Parasitol* **62**, 275 (1986).
- S7. D. W. Speicher, L. Weglarz, T. M. DeSilva, *J Biol Chem* **267**, 14775 (1992).
- S8. J. S. Arthur, J. S. Elce, C. Hegadorn, K. Williams, P. A. Greer, *Mol Cell Biol* **20**, 4474 (2000).
- S9. D. S. Roos, R. G. Donald, N. S. Morrissette, A. L. Moulton, *Methods Cell Biol* **45**, 27 (1994).
- S10. K. Hu *et al.*, *Mol Biol Cell* **13**, 593 (2002).
- S11. M. Matrajt, M. Nishi, M. J. Fraunholz, O. Peter, D. S. Roos, *Mol Biochem Parasitol* **120**, 285 (2002).
- S12. M. E. Fichera, M. K. Bhopale, D. S. Roos, *Antimicrob Agents Chemother* **39**, 1530 (1995).
- S13. B. Striepen, C. Y. He, M. Matrajt, D. Soldati and D. S. Roos, *Molec Biochem Parasitol* **92**, 328 (1998).